ELSEVIER

Journal of Alloys and Compounds 434–435 (2007) 348–353

Journal of ALLOYS AND COMPOUNDS

www.elsevier.com/locate/jallcom

Phase transformations study on $Ni_{75}Al_{25}$ and $Ni_{50}Al_{50}$ during mechanical alloying and sintering

L. D'Angelo [a], G. González [b,*], J. Ochoa [b]

[a] *Departamento de Mecánica, UNEXPO, Luis Caballero Mejías, Charallave, Venezuela*
[b] *Laboratorio de Ciencias e Ing. de Materiales, Dpto. Ingeniería, Instituto Venezolano de Investigaciones Científicas, Apdo. 21827, Caracas 1020A, Venezuela*

Available online 10 October 2006

Abstract

In the present work we study the phase transformations taking place by mechanical alloying in the Ni–Al system and with further consolidation by sintering at high pressures with the aim of maintaining nanometric grain size. Different phase transformations were observed during milling, a Ni(Al) saturated solid solution for Ni–25 at.%Al and the formation of the intermetallic compound for Ni–50 at.%Al. Amorphization and recrystallization was also observed after prolonged milling. These phases remain after sintering with nanometric grain size and very high values of hardness.

Keywords: Intermetallics; Nanostructure materials; Mechanical alloying; X-ray diffraction

1. Introduction

NiAl intermetallic compounds have low density, high strength and good corrosion and oxidation resistance. Mechanical alloying has been successfully applied to Ni–Al alloys by a number of authors [1–7]. These works show that the final structure obtained strongly depends on the milling process. Atzmon [1] established the occurrence of a self-sustaining reaction during ball milling for this system; this result was also confirmed by Cardellini et al. [3] However, Zbiral et al. [7] have proposed that, in general, alloying occurs by a diffusion mechanism of one element into the other but the mechanism is not totally clear. Paby and Murty [5] studying mechanical alloying of Ni_{50}–Al_{50} obtained evidence of formation of NiAl intermetallic compound after 8 h of milling but it was only after 20 h that the complete disappearance of elemental powders was observed. Ur and Nash [8] obtained complete transformation to the intermetallic compound NiAl after 61 h of milling. For compositions of Ni–25 at.%Al some authors [3,4] reported the formation of Ni(Al) supersaturated solid solution by mechanical alloying, however Pabi et al. [5] reported the presence of disordered Ni_3Al for this composition. Other authors have work on phase transformations of the intermetallic NiAl when adding a third element during milling [9–11]. Consolidation of the milled powders by hot pressing and by extrusion has also been carried out [12–15], the authors obtained high strength at room and elevated temperatures and good compressive ductility. They report a yield strength of 1200 MPa at room temperature for the mechanically alloyed consolidated powder compared to only 300 MPa for the as-cast alloy. High pressure torsion (HPT) consolidation techniques at room temperature have also been successfully employed [16] to obtain consolidated nanophase metallic compounds.

In the present work we performed mechanical alloying (MA) of the Ni–25 at.%Al and Ni–50 at.% elemental powders, from 1 to 50 h with the aim of studying the phase transformations taking place during the process. Consolidation by sintering at high pressures and intermediate temperature, of the powders milled for 5, 20 and 50 h, was carried out.

2. Experimental

Elemental high purity Ni powders, analytical grade, with an average particle size of 2 μm were mixed in a proportion of 50 at.% and 75 at.% with Al powders of particle size of 12 μm in a WAV turbule during 1 h and then mechanically alloyed under nitrogen atmosphere, using a SPEX 8000, for different milling periods, using vial and balls of stainless steel, and a ball-to-powder weight ratio (BPR) of 8:1. Sintering of the milled powders was performed at 700 °C and 2 GPa for 30 min in an uniaxial press equipped with a high temperature furnace. The characterization of powders and sintered material was carried out by X-

* Corresponding author. Tel.: +58 2125041430; fax: +58 2125041418.
E-mail addresses: patina@cantv.net (L. D'Angelo), gemagonz@ivic.ve (G. González).

0925-8388/$ – see front matter © 2006 Elsevier B.V. All rights reserved.
doi:10.1016/j.jallcom.2006.08.212

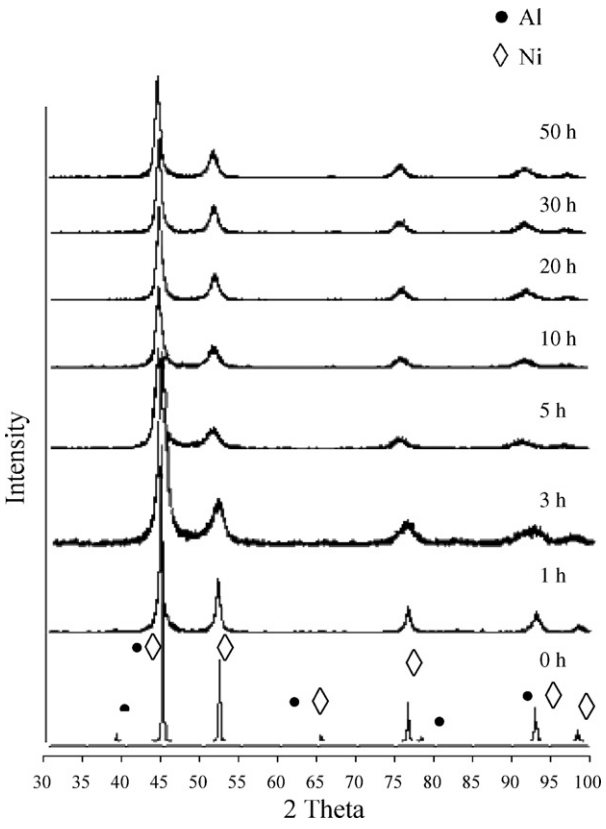

Fig. 1. XRD patterns of Ni–25 at.%Al powders milled from 1 to 50 h.

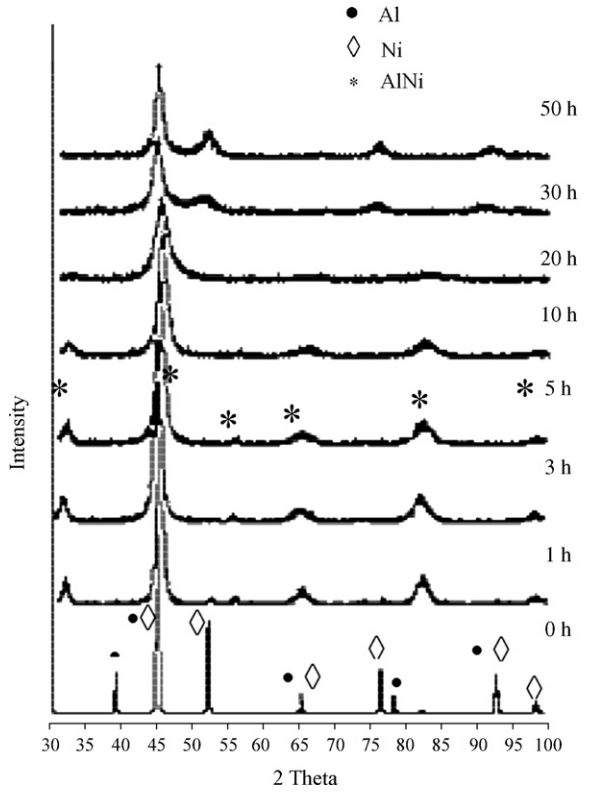

Fig. 2. XRD patterns of Ni–50 at.%Al powders milled from 1 to 50 h.

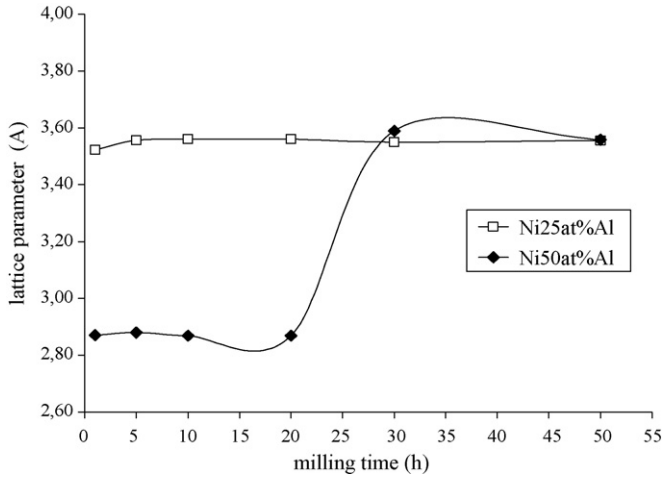

Fig. 3. Variation the lattice parameter for Ni–25 at.%Al and Ni–50 at.%Al with the milling time.

ray diffraction (XRD) using a Siemens 5005 diffractometer with Cu Kα. Grain size was calculated by the Scherrer equation. Scanning electron microscopy (SEM) analysis was performed in a Phillips XL30 attached with an EDX DX4. Transmission electron microscopy (TEM) was carried out in a Phillips CM10. Microhardness tests were performed to the sintered samples.

3. Results and discussion

The evolution of the transformations occurring during milling was followed by XRD, Figs. 1 and 2 show the diffraction patterns for Ni–25 at.% Al and Ni–50 at.% Al, respectively. The formation of a supersaturated solid solution was observed for Ni–25 at.%.Al from 1 h of milling up to 50 h, peak broadening and decrease in intensity was observed with milling time due to decreasing grain size, from 27 nm after 1 h to 7 nm after 5 h. However, a slight increase in grain size was observed with further milling reaching 9 nm after 50 h, this is consistent with the peak narrowing observed in the XRD pattern. Shifting of the main reflexion towards lower angles was observed, due to increase in lattice parameter from 3.523 Å after 1h of milling to

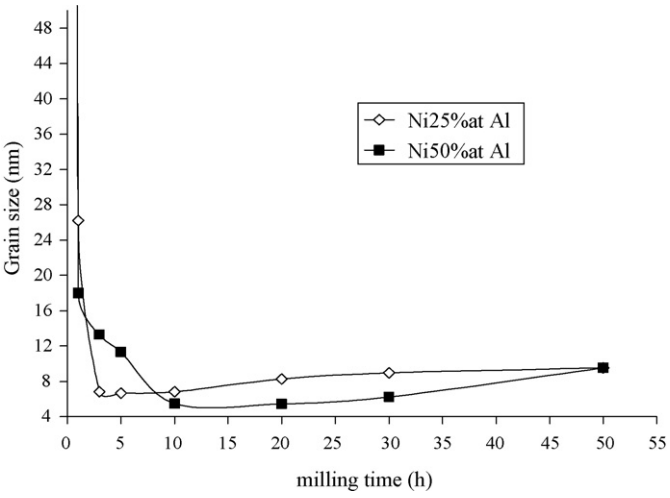

Fig. 4. Variation the grain size for Ni–25 at.%Al and Ni–50 at.%Al with the milling time.

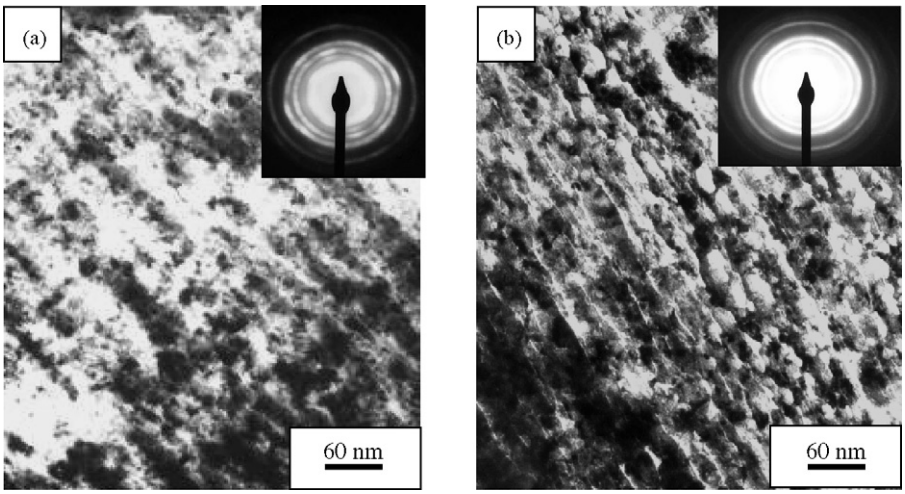

Fig. 5. Bright field images of Ni–25 at.%Al mechanically alloyed: (a) 5 h and (b) 50 h.

3.555 Å after 50 h, attributed to a distortion of the Ni lattice by diffusion of Al.

The XRD pattern for Ni–50 at.%Al show the formation of the intermetallic NiAl, after only 1 h of milling, with some Ni reflexions still present, complete transformation to NiAl intermetallic compound was observed after 5 h of milling, with a grain size of 11 nm. Further milling induces peak broadening to the extent that the structure becomes amorphous after 20 h; this was also observed by electron microscopy analysis. A partial phase transformation from amorphous to a supersaturated Ni(Al) solid solution was observed at 30 h of milling, which is completed at 50 h. The lattice parameter after 1 h of milling is 2.87 Å, corresponding to the value of the NiAl intermetallic compound, this value is maintained up to 20 h and from 30 h onwards increases to 3.55 Å, which is the expected value for Ni(Al) solid solution. The grain size decreases from 18 nm after 1 h of milling to 4 nm after 20 h, and then slightly increases with further milling to 9 nm after 50 h, due to crystallization and growth of the new phase formed. Figs. 3 and 4 show the variation in lattice parameter and grain size with milling time for both alloys.

Figs. 5 and 6 show the TEM bright field images and electron diffraction patterns of the Ni–25 at.%Al and Ni–50 at.%Al, respectively, milled 5 and 50 h. The electron diffraction pattern corresponding to Ni–25 at.%Al alloy milled 5 h shows spotty rings with some texture present, indicating the strong deformation in the material, also evident in the bright field image, however after 50 h of milling a very small uniform grain size was observed and by electron diffraction the formation of the Ni(Al) solid solution was confirmed. TEM analysis of Ni–50 at.%Al milled for 5 h and 50 h revealed the presence of the intermetallic compound NiAl consistent with XRD results and a very small and uniform grain size after 50 h of milling is observed in the bright and dark field images (Fig. 6b). The analysis of the material milled 20 h reveals an amorphous structure in the electron diffraction pattern (Fig. 7a), however this sample after a few seconds under the electron beam radiation begins to crystallize *in situ*, as can be observed in the sequence of electron diffraction patterns taken with a few seconds intervals to the same sample area (Fig. 7b–c), crystallization is completed after approximately 2 min of electron beam radiation. This phenomenon is an indication of the high deformation energy accumulated in

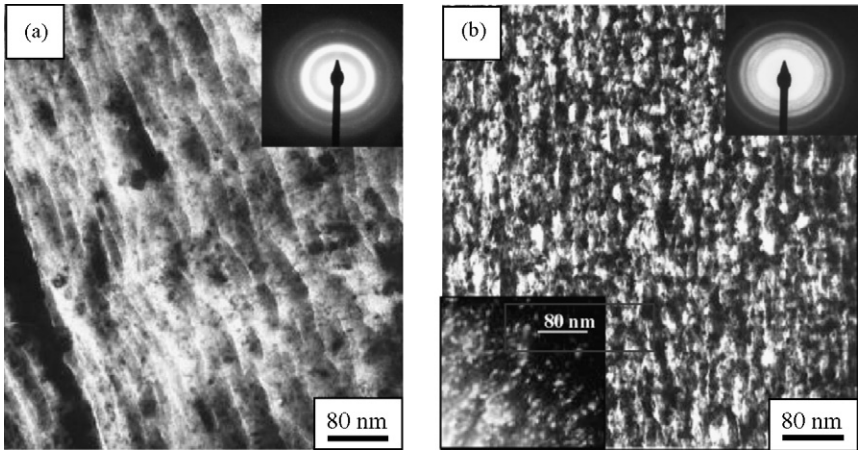

Fig. 6. TEM images of Ni–50 at.%Al mechanically alloyed (a) 5 h, bright field image (b) 50 h, bright and dark field in the inset.

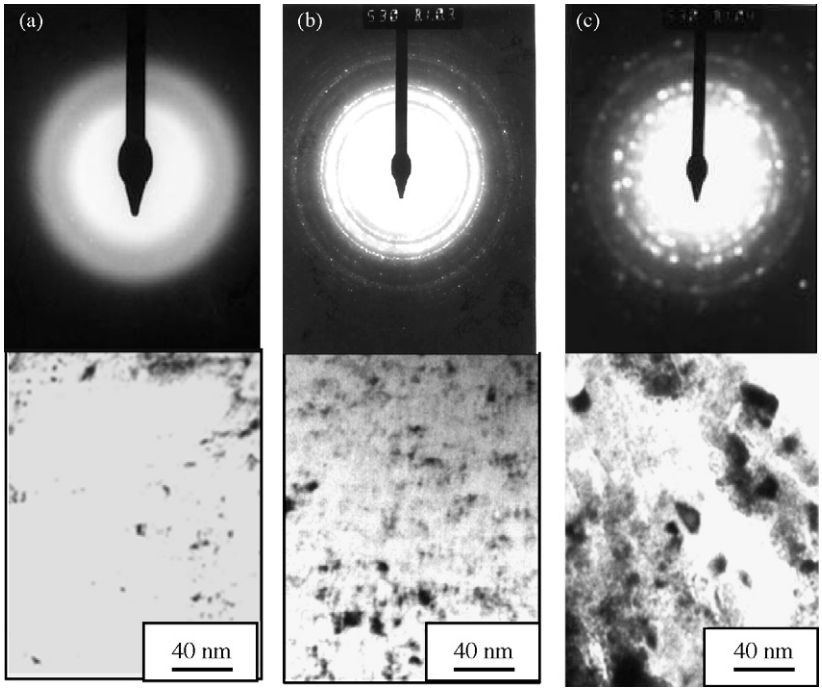

Fig. 7. Bright field images with their respective electron diffraction patterns of Ni–50 at.%Al mechanically alloyed 20 h. Micrographs were taken in sequence with a few seconds intervals of sample exposure under the electron beam radiation.

the material and could explain the crystallization of this alloy observed after prolonged milling from 20 h onward. The XRD patterns of the powders milled and sintered for both alloys are compared in Figs. 8 and 9. Ni–25 at.%Al did not suffer any phase transformation during the sintering process for any of the milled samples, Ni(Al) solid solution was obtained for all the cases, only a small increase in the grain size was observed from 7 nm in the 5 h milled powder to 19 nm after sintering and for the 50 h milled powders from 9 to 28 nm. It is interesting to notice the very small increase in grain size obtained after sintering probably due to the very high pressures used in this process helping consolidation without the need of prolonged treatments at high temperature, resulting in a nanometric bulk material.

Ni–50 at.%Al (Fig. 9) show an increase in grain size from 11 to 32 nm after sintering. The 20 h milled alloy is almost completely amorphous however after sintering the formation of the nanometric NiAl intermetallic compound is observed with a grain size of 7 nm. Analogously, it has been recently reported that high-pressure torsion can be used to compact amorphous ribbons [17]. In the sample previously milled 50 h and sintered the Ni(Al) solid solution was preserved with a grain size of 18 nm, also small amounts of the NiAl intermetallic compound were obtained. The variation of grain size with sintering for the different milled powders is shown in Table 1. These values are much lower than those reported for NiAl MA consolidated by different methods [12–16]. Microhardness measurements performed in the sintered materials are shown in Table 2, the values obtained are in the range of 1000–900 Hv, these are very high compared those reported for hot pressed and vacuum hot pressed materials [11], the highest values are observed for the sintered alloys previously milled 5 h. The hardness value for the alloy Ni–50 at.%Al milled 5 h and sintered is slightly higher than for the 25 at.%Al. The values obtained in the samples milled 50 h

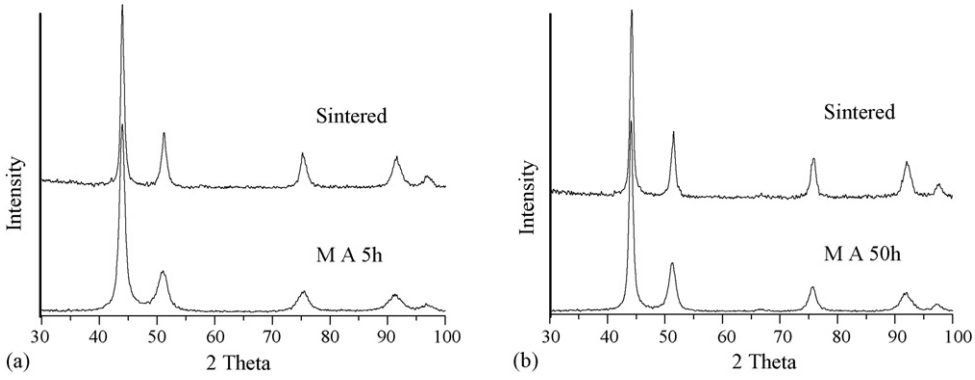

Fig. 8. XRD Ni–25 at.%Al mechanical alloyed (MA) and sintered at 2 GPa and 700 °C.

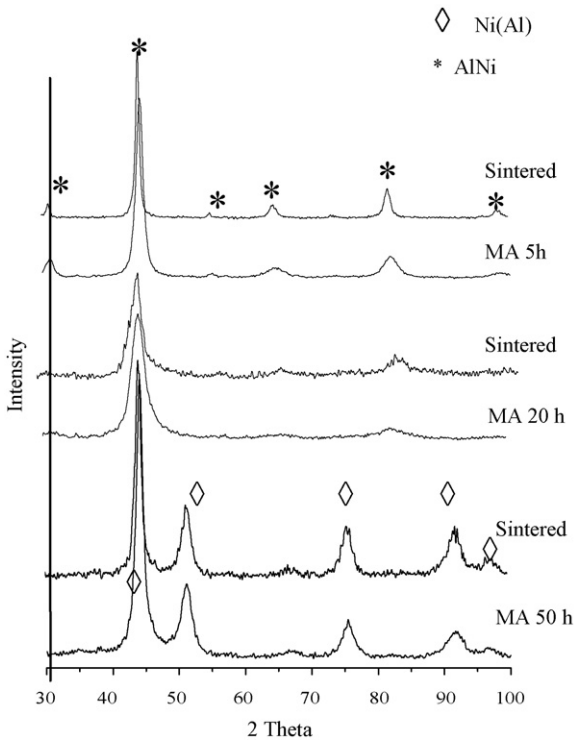

Fig. 9. XRD Ni–50 at.%Al after mechanical alloying (MA) and Sintering at 2 GPa and 700 °C.

Table 1
Variation the grain size values for Ni–25 at.%Al and Ni–50 at.%Al Alloys with milling for different periods and sintering

Milling time (h)	Process	Grain size (nm)	
		Ni–50 at.%Al	Ni–25 at.%Al
5	Milling	11	7
	Sintering	32	19
20	Milling	5	–
	Sintering	7	–
50	Milling	9	9
	Sintering	18	28

and sintered are slightly lower, probably due to a better sintering process in the samples milled for 5 h.

SEM micrographs of the sintered samples of both alloys are observed in Figs. 10 and 11. The 5 h milled samples show a better consolidation with less apparent porosity in the images. This

Table 2
Microhardeness values after sintering for Ni–25 at.%Al and Ni–50 at.%Al

%Al	Milling time (h)	Sintering conditions	Microhardness (HV)
25	5	2 GPa, 700 °C	1004
25	50	2 GPa, 700 °C	913
50	5	2 GPa, 700 °C	1050
50	20	2 GPa, 700 °C	961
50	50	2 GPa, 700 °C	961

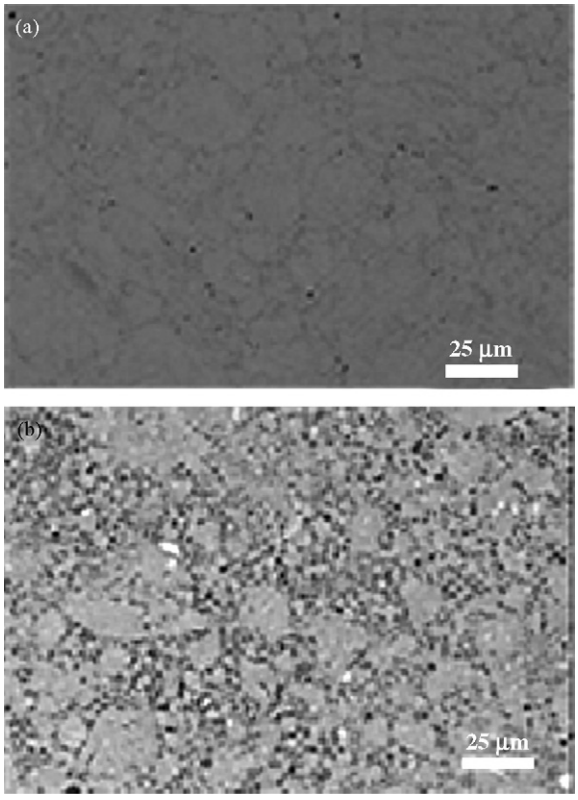

Fig. 10. SEM images Ni–25 at.%Al powders sintered at 2 GPa and temp. 700 °C after MA (a) 5 h and (b) 50 h.

can be due to the sintering mechanism of mechanically alloyed powders, in which the agglomerate size controls the sintering process. After 5 h of milling the size of agglomerates has a wider distribution than for 50 h and this seems to help the sintering process. TEM analysis of the sintered samples showed nanometric grain size with a very uniform distribution, a bright field image and diffraction pattern of the sintered materials milled 50 h is

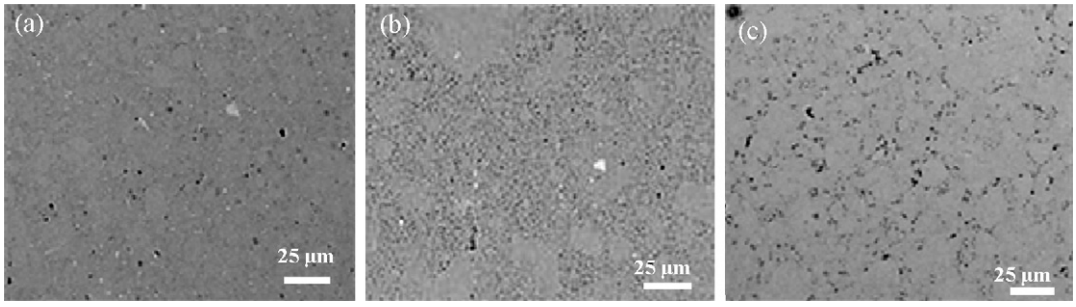

Fig. 11. SEM images Ni–50 at.%Al powders sintered at 2 GPa and temp. 700 °C after MA (a) 5 h (b) 20 h and (c) 50 h.

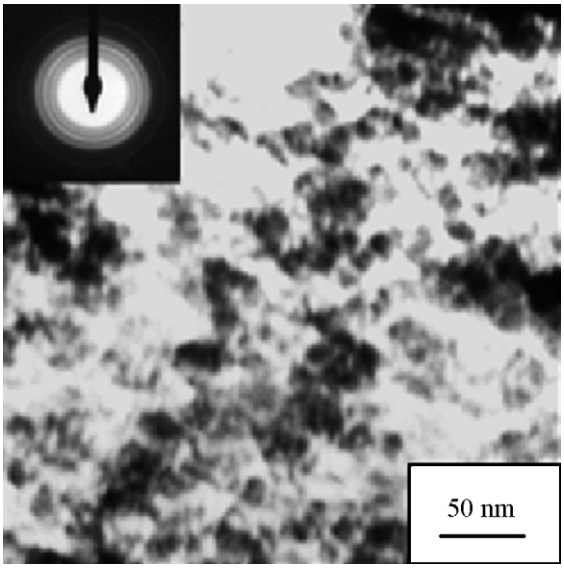

Fig. 12. Bright field images of Ni–50 at.%Al milled 50 h and sintered at 2 GPa and 700 °C.

shown in Fig. 12, in very good agreement with the XRD measurements.

4. Conclusions

The formation of Ni(Al) solid solution is observed alter 5 h of milling up to 50 h for the Ni–25 at.%Al. For the Ni–50 at.%Al the formation of NiAl intermetallic compound is observed after 1 h of milling and is completely formed after 5 h. This alloy amorphizes after 20 h of milling and with further milling crystallization to a new solid solution is observed with the formation of a small amount of Ni_3Al.

Sintering of both alloys previously milled for different periods show nanometric grain size with very high microhardness values in the range of 1000–900 Hv.

References

[1] M. Atzmon, Phys. Rev. Lett. 64 (1988) 487–490.
[2] E. Ivanov, T. Grigorieva, G. Golubkova, V. Boldyrev, A.B. Pasman, S.D. Mikhailenko, O.T. Kalinina, Mater. Lett. 7 (1–2) (1988) 51–54.
[3] F. Cardellini, F. Cleri, G. Mazzone, A. Montone, V. Rosato, J. Mater. Res. 8 (1993) 2504–2509.
[4] F. Cardellini, G. Mazzone, A. Montone, M. Victtori Antisari, Acta Metall. Mater. 42 (7) (1994) 2445–2451.
[5] S.K. Pabi, B.S. Murty, Mater. Sci. Eng. A214 (1996) 146–152.
[6] B.S. Murty, k.S. Singh, S.K. Pabi, Bul. Mater. Sci. 19 (3) (1996) 565–571.
[7] J. Zbiral, G. Jangg, G. Knorb, Mater. Sci. Forum 88–90 (1992) 19–24.
[8] S.C. Ur, P. Nash, Metall. Mater. Trans. A 25A (1994) 871–874.
[9] A.M. Blinov, V.K. Portnoy, S.D. Kaloshkin, I.A. Tomilin, J. Metast. Nanocrys. Mater. 20–21 (2004) 151–156.
[10] Z.G. Liu, J.T. Guo, L.Z. Zhou, Z.Q. Hu, M. Umemoto, J. Mater. Sci. 32 (18) (1997) 4857–4864.
[11] A. Antolak, M. Krasnowski, T. Kullik, Rev. Adv. Sci. 8 (2004) 111–115.
[12] S.G. Pyo, N.J. Kim, P. Nash, Mater. Sci. Eng. A181/A182 (1994) 1169–1173.
[13] S.C. Ur, P. Nash, G.T. Higgins, Scripta Mater. 34 (1) (1996) 53–59.
[14] S. Dymek, M. Dollar, S.J. Higgins, P. Nash, Mater. Sci. Eng. A 152 (1992) 160–165.
[15] S. Suh, M. Dollar, P. Nash, Mater. Sci. Eng. A192/A193 (1995) 691–697.
[16] J. Sort, D.C. Lle, A.O. Zhilyaev, A. Concustell, T. Czeppe, M. Stoica, S. Suriñac, J. Eckert, M.D. Baro, Scripta Mater. 50 (2004) 1221–1225.
[17] J. Sort, A. Zhilyaev, M. Zelinska, J. Noguès, S. Suriñac, J. Thibault, M.D. Baro, Acta Mater. 51 (2003) 6385–6393.